Effects of basal-melting distribution on the retreat of ice-shelf grounding lines

R. T. Walker,[1] T. K. Dupont,[2] B. R. Parizek,[3] and R. B. Alley[1]

Received 6 June 2008; revised 10 July 2008; accepted 22 July 2008; published 5 September 2008.

[1] The stability of marine ice streams depends on the distribution as well as the magnitude of melting beneath the adjacent ice shelf, as shown by new model results. Recent observations of rapid retreat of ice-shelf grounding lines in the Amundsen Sea sector of West Antarctica have highlighted the need for understanding how basal melting of ice shelves by warm ocean waters affects ice dynamics and potentially contributes indirectly to sea-level rise. We apply two ice stream-ice shelf flow line models to investigate the effects of varying the spatial distribution of basal melting on grounding-line dynamics. For experiments with identical average melting, we find that retreat increases significantly as melting is concentrated near the grounding line, indicating that knowledge of the basal-melting distribution is likely necessary for accurate prediction of grounding-line migration. **Citation:** Walker, R. T., T. K. Dupont, B. R. Parizek, and R. B. Alley (2008), Effects of basal-melting distribution on the retreat of ice-shelf grounding lines, *Geophys. Res. Lett.*, *35*, L17503, doi:10.1029/2008GL034947.

1. Introduction

[2] Ice shelves, the floating extensions of outlet glaciers and ice streams that drain the Greenland and Antarctic ice sheets, have the potential to significantly affect sea level. Although melting of already-floating ice would have little direct effect upon sea-level rise, ice shelves play an important role in buttressing the flow of inland ice [*Dupont and Alley*, 2005, 2006], with their reduction or loss leading to acceleration of tributary glaciers [*Scambos et al.*, 2004]. The stability of the West Antarctic Ice Sheet (WAIS), which rests upon a bed mostly below sea level, has been of particular concern for some time [*Weertman*, 1974; *Thomas*, 1979; *Hughes*, 1980; *Thomas et al.*, 2004]. The ice shelves of the Amundsen Sea sector of WAIS have recently experienced notable increase in basal melting due to the incursion of warm Circumpolar Deep Water (CDW) into sub-shelf cavities, resulting in considerable thinning and grounding-line retreat [e.g., *Jenkins et al.*, 1997; *Shepherd et al.*, 2004].

[3] Assessing basal melting of ice shelves and predicting the response of inland ice is thus a modeling problem of some interest. Hydrographic measurements taken from ships near ice fronts, combined with tracer conservation models, yield estimates of total basal melting for particular sub-shelf cavities [*Jacobs et al.*, 1996; *Jenkins and Jacobs*, 2008]. However, such methods do not provide information about the spatial distribution of melting, which models [*Payne et al.*, 2007; *Walker and Holland*, 2007] and observations [*Rignot and Jacobs*, 2002] suggest is concentrated relatively near grounding lines. In situ measurements by phase-sensitive radar atop ice shelves [*Corr et al.*, 2002; *Jenkins et al.*, 2006] or autonomous submersibles below them [*Price et al.*, 2008] would likely be needed to obtain this information. In this study, we therefore apply two ice stream-ice shelf flow line models to investigate whether knowledge of the distribution of basal melting is necessary for accurate prediction of grounding-line migration.

2. Methods

[4] This study primarily uses a version of the *Dupont and Alley* [2005] ice stream-ice shelf model, as modified for eventual incorporation into the coupled ice-ocean framework of *Walker and Holland* [2007]. This version differs from the original in that it is dimensional, that the mass balance includes basal melting, and that the equations are solved by finite-difference methods on a staggered grid. The model solves for the thickness $h(x, t)$ and velocity $u(x, t)$ of an ice stream flowing through a parallel-sided channel from $x = 0$ to $x = L_x$. For simplicity, we assume that the channel has a constant width $2L_y$, and a bed elevation given by $z_r(x) = z_0 + \beta x$, where $z_r = 0$ at sea level. It follows that $h_f(x) = -(\rho_w/\rho_i)\, z_r(x)$ is the maximum thickness of floating ice; we will identify the point x_g at which $h(x_g) = h_f(x_g)$, found by interpolation, as the grounding line.

[5] The depth-integrated, width-averaged momentum balance is given by

$$\partial_x\left(4h\nu\partial_x u - \frac{\rho_i g}{2}h^2\right) = \rho_i g h \partial_x z_b + \frac{h}{L_y}T_y(u) + T_b(u) \quad (1)$$

where ρ_i, ρ_w denote the densities of ice and seawater, respectively, and $z_b(x, t) = \max(z_r, -(\rho_i/\rho_w)h)$ is the depth of the ice base. The effective viscosity ν is defined as

$$\nu \equiv \frac{B}{2}|\partial_x u|^{-\frac{1}{3}} \quad (2)$$

where $B = A^{-1/3}$ is the ice hardness parameter and A is the ice softness parameter in Glen's law. The lateral drag is given by

$$T_y = \tau_y u^{\frac{1}{3}} \quad (3)$$

[1] Earth and Environmental Systems Institute and Department of Geosciences, Pennsylvania State University, University Park, Pennsylvania, USA.
[2] Department of Earth System Science, University of California, Irvine, California, USA.
[3] Mathematics and Geoscience, Pennsylvania State University, DuBois, Pennsylvania, USA.

0094-8276/08/2008GL03494

and the basal drag by

$$T_b = \begin{cases} \tau_b u, & h > h_f \\ 0, & h \le h_f \end{cases} \quad (4)$$

where τ_y and τ_b are constant coefficients. Our choices of power-law exponents are consistent with lateral and basal drag derived from shearing of ice and softer sediment (e.g., till), respectively. The velocity at the upstream end is derived from the prescribed flux, q_0, so that $u(0, t) = q_0/h(0, t)$. At the downstream end, we prescribe the buttressing boundary condition

$$\left[4h\nu\partial_x u - \frac{\rho_i g}{2}h^2\right]_{x=L_x} = \left[-f\frac{\rho_i g}{2}h^2 - (1-f)\frac{\rho_w g}{2}z_b^2\right]_{x=L_x} \quad (5)$$

which is a linear combination of the unbuttressed ($f = 0$) condition appropriate to an ice front or freely-floating ice shelf and the fully-buttressed ($f = 1$) condition for which the longitudinal deviatoric stress is zero.

[6] The mass balance is given by the continuity equation

$$\partial_t h = -\partial_x(uh) - m, \quad (6)$$

where we neglect surface accumulation or ablation so that the only forcing is the basal melt rate m. The flux at the upstream end is a prescribed constant, $q_0 = q(0, t)$. This simplification is adequate for the present idealized study; specification of a time-dependent flux would depend upon the geometry and/or transient surface mass balance of a particular catchment, and will be considered in future work. As we cannot specify another boundary condition at $x = L_x$, ice is allowed to advect freely out of the domain.

[7] The initial configuration for all experiments is derived by running the model to equilibrium in the absence of basal melting, with parameter values as shown in Table 1. We note that identical final states are obtained from an arbitrary fully-grounded initial condition; however, using the zero-melt steady state as the initial condition allows us to attribute changes in the system to ice-ocean interaction. While qualitatively similar results are obtained at coarser resolution, the model is run with a time step of one day and a grid spacing of 100 m in order to minimize numerical artifacts affecting grounding-line migration [*Vieli and Payne*, 2005]. The lateral friction coefficient τ_y is adjusted to produce a 50 km shelf and a 100 km stream; as the domain geometry and input fluxes are identical, this configuration is essentially the buttressed experiment of *Dupont and Alley* [2005] with an explicitly-appended ice shelf replacing the buttressing boundary condition. (The explicit ice shelf is equivalent to setting the buttressing parameter $f = 0.49$, compared with $f = 0.5$ in the original experiment.) We note that this initial configuration is representative of the Amundsen Sea ice shelves, such as Pine Island Glacier, but does not attempt to simulate any particular ice shelf.

[8] In order to study the effect of the distribution of basal melting on grounding-line migration, experiments are run using a variety of melt profiles with the same average melt rate $\bar{m}$ (Figure 1). The profiles are given by

$$m = \frac{\bar{m}}{N}\left(1 - \frac{x - x_g}{L_x - x_g}\right)^{\alpha-1}\left(\frac{x - x_g}{L_x - x_g}\right)^{\beta-1}, \quad (7)$$

where $x_g \le x \le L_x$ and N is a normalization factor defined so that $(L_x - x_g)^{-1}\int_{x_g}^{L_x} m dx = \bar{m}$. The parameters (α, β) control the shape of the melting distribution; note that m is a constant function for $(\alpha, \beta) = (1, 1)$, linear for (2, 1), and quadratic for (3, 1). These simplified, arbitrary profiles are chosen to reflect the tendency of basal melting to peak near the grounding line [e.g., *Rignot and Jacobs*, 2002; *Walker and Holland*, 2007; *Payne et al.*, 2007], with the assumption of constant melting serving as a control. Basal melting is applied to all floating ice, allowing for partial cells when the grounding line lies between grid points, with the profiles allowed to stretch such that the average melt rate remains constant. The experiments are repeated for average melt rates of 5, 10, and 15 m/yr, which are consistent with the 12 ± 3 m/yr estimated for Pine Island Glacier by *Jenkins et al.* [1997]. We note that *Payne et al.* [2007] calculated significantly higher melting; however, the melt rates used in this study are sufficiently large to illustrate the relevant processes.

Table 1. Values of Constants and Parameters

Constant or parameter	Value
ρ_i	917 kg m^{-3}
ρ_w	1028 kg m^3
L_y	20 km
L_x	150 km
z_0	−1192 m
β	3.0×10^{-3}
τ_y	2.63×10^6 Pa m$^{-1/3}$ s$^{1/3}$
τ_b	1.0×10^9 Pa m^{-1} s
q_0	7.6×10^{-2} m^2 s^{-1}
A	4.9×10^{-25} s^{-1} Pa^{-3}

3. Results

[9] All of the experiments with an average melt rate of 5 m/yr result in grounding-line retreat to new steady positions within 500 years (Table 2). (For purposes of this study, we set our steady-state criterion as no grounding-line migration for 500 years.) The extent of the retreat and the concomitant loss of volume above flotation (VAF) vary, from the constant profile retreating 6.8 km and losing 14% of initial VAF to the quadratic profile retreating 11.1 km and losing 22% of initial VAF. Conversely, all of the experiments with an average melt rate of 15 m/yr (Table 3) result in flotation of the entire initial ice stream (i.e., loss of 100% of initial VAF), with the time required to do so ranging from 335 years for the constant profile to only 150 years for the quadratic profile (Table 3). While the applied boundary conditions require that all fully-retreated final states are identical, this large variation in the speed of grounding-line retreat would likely be significant for sea-level prediction. The strongest dependence of grounding-line retreat on basal-melting distribution occurs in the experiments with an average melt rate of 10 m/yr (Figure 2), for which the

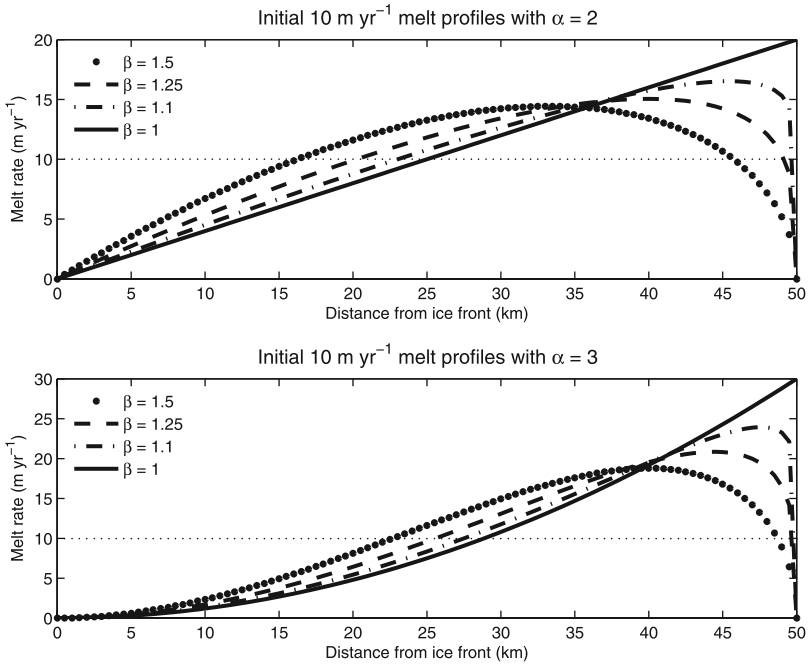

Figure 1. Examples of imposed basal melting profiles. Note differing vertical scales. Average value (dotted line) shown for reference.

profile used can make the difference between reaching a new steady position and flotation of the entire domain. For example, the constant profile retreats 21.2 km, largely in the first 300 years, and then holds steady; however, the quadratic profile results in flotation of the entire domain in 445 years. Extended runs show that the (α, β) = (2, 1.5) and (2, 1.25) experiments become steady after 30.7 and 41.3 km of retreat, respectively, while the (2, 1.1) profile floats the entire domain in 1385 years. We further note that although the domain of the present study is relatively small, Figure 2 and the 15 m/yr experiments show that the rates of grounding-line retreat are typically increasing rapidly as the edge of the domain is approached, suggesting that retreat would have continued had the boundary not been reached.

[10] The evolution of the system is controlled by the interplay between spatially-varying basal melting and velocity-dependent lateral drag, which is particularly significant for relatively thick and narrow ice streams. In order to isolate sensitivity of the system to melt distribution, we hold all other dynamic parameters constant (cf. shear-margin weakening, etc. [*Vieli et al.*, 2007]). Comparison of the initial (no basal melting) and final steady states (Figure 3) shows that the ice shelf slows as it lengthens and thins, while the ice stream accelerates due to loss of basal friction downstream as the grounding line retreats. The base of the ice shelf becomes steeper near the grounding line and flatter towards the ice front, leading to greater loss of velocity as the ice front is approached; this effect becomes stronger as the imposed melting is concentrated near the grounding line. As the grounding line retreats, ice thickness h_g increases there, while the corresponding velocity v_g decreases (Table 2). The increase in h_g is a direct consequence of the sloping bed, for which the flotation thickness h_f increases in the upstream direction. Due to greater driving stress, an increase in v_g might be expected; however, increased buttressing more than compen-

Table 2. Summary of Final States of Experiments Resulting in Steady Grounding Line[a]

Experiment ($\bar{m}$, α, β)	Δ GL (km)	h_g (m)	v_g (m yr^{-1})	$\int \frac{h}{L_y} T_y$ (10^8 Pa m)	f_g	VAF
Initial	0	998.5	2367	2.380	.4915	1.000
(5, 1, 1)	6.79	1021.3	2314	2.615	.5161	.863
(5, 2, 1.5)	7.87	1025.0	2306	2.649	.5192	.841
(5, 2, 1.25)	8.49	1027.0	2302	2.671	.5213	.830
(5, 2, 1.1)	9.09	1029.1	2297	2.694	.5239	.818
(5, 2, 1)	9.59	1030.7	2293	2.715	.5262	.809
(5, 3, 1.5)	9.29	1029.7	2296	2.698	.5260	.815
(5, 3, 1.25)	9.89	1031.8	2291	2.720	.5293	.803
(5, 3, 1.1)	10.59	1034.1	2286	2.749	.5293	.790
(5, 3, 1)	11.09	1035.8	2282	2.770	.5315	.781
(10, 1, 1)	21.19	1069.7	2210	3.124	.5621	.607
(10, 2, 1.5)	30.69	1101.7	2146	3.462	.5873	.464
(10, 2, 1.25)	41.29	1137.4	2078	3.859	.6143	.329

[a]Experiments are labeled by average melt rate $\bar{m}$ and distribution parameters α, β.

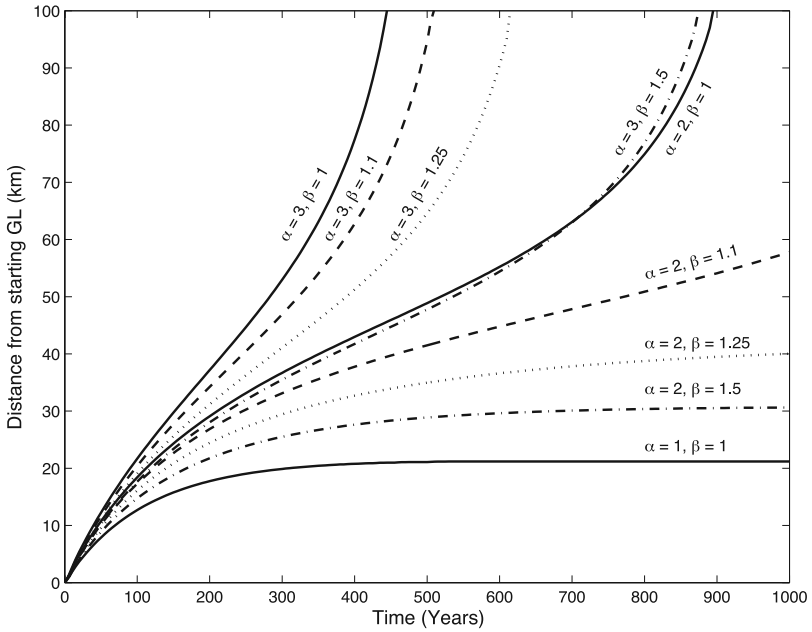

Figure 2. Grounding-line retreat for experiments with 10 m/yr average melt rate.

sates for this forcing. The effective buttressing at the grounding line, given by

$$f_g = 1 - \frac{4h\nu\partial_x u}{\frac{\rho_i g}{2}\left(1-\frac{\rho_i}{\rho_w}\right)h_g^2} = \frac{\int_{GL}^{L_x}\frac{h}{L_y}T_y dx}{\frac{\rho_i g}{2}\left(1-\frac{\rho_i}{\rho_w}\right)h_g^2} \quad (8)$$

as the ratio of lateral drag to depth-integrated hydrostatic pressure, increases over time (Table 2). This is a consequence of lengthening the shelf by addition of thicker floating ice near the new grounding line, since the integrated lateral drag at any fixed x actually decreases as the shelf thins and slows. However, the effective buttressing at the original grounding line also increases over time, since thinning causes the hydrostatic term to decrease faster than the lateral drag term. It would thus appear that the effects of basal melting cannot be simply parameterized as a loss of buttressing. We note that this increase in buttressing is a conservative result, as the freely-floating ice front remains either at or beyond the end of our domain such that the shelf is always lengthening with grounding-line retreat; ice-front retreat into our embayment would reduce lateral drag, likely reducing buttressing and increasing the rate of grounding-line retreat.

[11] In order to confirm these results, some of the experiments were repeated using the higher-order Parizek model [*Alley et al.*, 2007], with global resolution of 1 km refined to 100 m near the grounding line. The inclusion of vertically-varying stresses in this model leads to a softening of the ice relative to the vertically-integrated Dupont model; it follows that the initial steady state of the Parizek model without basal melting consists of a slightly longer (approximately 55 km) shelf with a correspondingly deeper grounding line. The softening effect likewise contributes to a stronger grounding-line response to basal melting in the Parizek model (e.g., an additional 10.6 km of retreat for the constant 10 m/yr experiment). Despite differences in physics, however, both models display similar sensitivity to the distribution of basal melting, with a constant-melting profile producing a new steady grounding-line position but profiles concentrated towards the grounding line leading to flotation of the entire domain. This qualitative agreement between models increases our confidence in these results.

Table 3. Experiments Resulting in Flotation of Entire Ice Stream[a]

Experiment ($\bar{m}$, α, β)	Time to flotation (years, rounded)
(10, 2, 1.1)	1385
(10, 2, 1)	895
(10, 3, 1.5)	874
(10, 3, 1.25)	615
(10, 3, 1.1)	509
(10, 3, 1)	445
(15, 1, 1)	335
(15, 2, 1.5)	230
(15, 2, 1.25)	205
(15, 2, 1.1)	190
(15, 2, 1)	180
(15, 3, 1.5)	180
(15, 3, 1.25)	165
(15, 3, 1.1)	155
(15, 3, 1)	150

[a]Experiments are labeled by average melt rate $\bar{m}$ and distribution parameters α and β.

4. Conclusions

[12] In our experiments, the average basal melt rate exerts the greatest influence over grounding-line retreat. However, in experiments with the same average melting, significantly different results are obtained as this melting is concentrated near the grounding line. We further note that the decrease in the local freezing point of seawater with depth would tend to increase the thermal forcing due to penetration of warm CDW as the grounding line retreats upstream along an inland-sloping bed, so that the steady imposed melting profiles used in this study may well underestimate this effect. Given that we have applied somewhat arbitrary forcing to models of reduced dimension, our results should

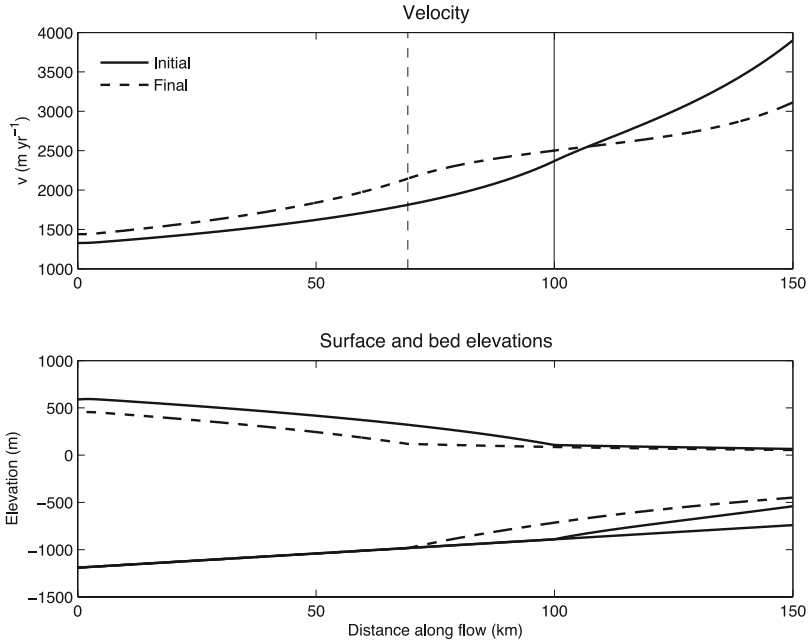

Figure 3. Comparison of initial and final steady states for ($\bar{m}$, α, β) = (10, 2, 1.5) experiment. Vertical lines in velocity subplot indicate grounding line positions.

not be taken as definitive predictions. Nevertheless, we have demonstrated qualitatively similar behavior in two models of differing complexity, implying that sensitivity to basal-melting distribution is an effect which should be considered in future modeling studies. Our results thus suggest that accurate prediction of grounding-line retreat for ice shelves undergoing high basal melting requires knowledge of the distribution of this melting, indicating the potential for detailed field observations to play an important role in assessing the contribution of the West Antarctic Ice Sheet to sea-level rise.

[13] **Acknowledgments.** R. T. Walker and R. B. Alley were supported by the Center for Remote Sensing of Ice Sheets (CReSIS). We also thank the Gary Comer Science and Education Foundation for support. T. K. Dupont was supported by NSF grants 0809106 and 0814241. B. R. Parizek was supported by NSF grants 0531211 and 0758274, and by NASA grant NRA-04-OES-02. We appreciate helpful comments by J. N. Bassis and an anonymous reviewer, as well as productive discussions among members of the PSICE center at Penn State.

References

Alley, R. B., et al. (2007), Effect of sedimentation on ice-shelf grounding-line stability, *Science*, *315*, 1838–1841.

Corr, H. F. J., A. Jenkins, K. W. Nicholls, and C. S. M. Doake (2002), Precise measurement of changes in ice-shelf thickness by phase-sensitive radar to determine basal melt rates, *Geophys. Res. Lett.*, *29*(8), 1232, doi:10.1029/2001GL014618.

Dupont, T. K., and R. B. Alley (2005), Assessment of the importance of ice-shelf buttressing to ice-sheet flow, *Geophys. Res. Lett.*, *32*, L04503, doi:10.1029/2004GL022024.

Dupont, T. K., and R. B. Alley (2006), Role of small ice shelves in sea-level rise, *Geophys. Res. Lett.*, *33*, L09503, doi:10.1029/2005GL025665.

Hughes, T. J. (1980), The weak underbelly of the West Antarctic Ice Sheet, *J. Glaciol.*, *27*, 518–525.

Jacobs, S. S., H. H. Hellmer, and A. Jenkins (1996), Antarctic Ice Sheet melting in the Southeast Pacific, *Geophys. Res. Lett.*, *23*, 957–960.

Jenkins, A., and S. Jacobs (2008), Circulation and melting beneath George VI Ice Shelf, Antarctica, *J. Geophys. Res.*, *113*, C04013, doi:10.1029/2007JC004449.

Jenkins, A., et al. (1997), Glaciological and oceanographic evidence of high melt rates beneath Pine Island Glacier, West Antarctica, *J. Glaciol.*, *43*, 114–121.

Jenkins, A., et al. (2006), Interactions between ice and ocean observed with phase-sensitive radar near an Antarctic ice-shelf grounding line, *J. Glaciol.*, *52*, 325–346.

Payne, A. J., P. R. Holland, A. P. Shepherd, I. C. Rutt, A. Jenkins, and I. Joughin (2007), Numerical modeling of ocean-ice interactions under Pine Island Bay's ice shelf, *J. Geophys. Res.*, *112*, C10019, doi:10.1029/2006JC003733.

Price, M. R., K. J. Heywood, and K. W. Nicholls (2008), Ice-shelf-ocean interactions at Fimbul Ice Shelf, Antarctica from oxygen isotope ratio measurements, *Ocean Sci.*, *4*, 89–98.

Rignot, E., and S. Jacobs (2002), Rapid bottom melting widespread near Antarctic Ice Sheet grounding lines, *Science*, *296*, 2020–2023.

Scambos, T. A., J. A. Bohlander, C. A. Shuman, and P. Skvarca (2004), Glacier acceleration and thinning after ice shelf collapse in the Larsen B embayment, Antarctica, *Geophys. Res. Lett.*, *31*, L18402, doi:10.1029/2004GL020670.

Shepherd, A., D. Wingham, and E. Rignot (2004), Warm ocean is eroding West Antarctic Ice Sheet, *Geophys. Res. Lett.*, *31*, L23402, doi:10.1029/2004GL021106.

Thomas, R. H. (1979), The dynamics of marine ice sheets, *J. Glaciol.*, *24*, 167–177.

Thomas, R., et al. (2004), Accelerated sea-level rise from West Antarctica, *Science*, *306*, 255–259.

Vieli, A., and A. J. Payne (2005), Assessing the ability of numerical ice sheet models to simulate grounding line migration, *J. Geophys. Res.*, *110*, F01003, doi:10.1029/2004JF000202.

Vieli, A., A. J. Payne, A. Shepherd, and Z. Du (2007), Causes of pre-collapse changes of the Larsen B ice shelf: Numerical modelling and assimilation of satellite observations, *Earth Planet. Sci. Lett.*, *259*, 297–306, doi:10.1016/j.epsl.2007.04.050.

Walker, R. T., and D. M. Holland (2007), A two-dimensional coupled model for ice shelf-ocean interaction, *Ocean Modell.*, *17*, 123–139.

Weertman, J. (1974), Stability of the junction of an ice sheet and an ice shelf, *J. Glaciol.*, *13*, 3–11.

R. B. Alley and R. T. Walker, Earth and Environmental Systems Institute and Department of Geosciences, Pennsylvania State University, 534 Deike Building, University Park, PA 16802, USA. (ralley@geosc.psu.edu; rwalker@geosc.psu.edu)

T. K. Dupont, Department of Earth System Science, University of California, 3204 Croul Hall, mail code 3100, Irvine, CA 92697, USA. (tdupont@uci.edu)

B. R. Parizek, Mathematics and Geoscience, Pennsylvania State University, 181 Smeal Building, College Place, DuBois, PA 15801, USA. (parizek@geosc.psu.edu)